A single molecule magnet (SMM) with a helicate structure†

Ghenadie Novitchi,[a] Jean-Pierre Costes,*[b] Jean-Pierre Tuchagues,[b] Laure Vendier[b] and Wolfgang Wernsdorfer*[c]

Received (in Montpellier, France) 23rd October 2007, Accepted 27th November 2007
First published as an Advance Article on the web 5th December 2007
DOI: 10.1039/b716283a

The X-ray structure determination of $[L_2Cu_2Gd_2(NO_3)_6(H_2O)_2]$-$(0.5H_2O)$ (L = bis-[(2-hydroxy-3-ethoxyphenyl)methylene]-4,4′-methylenedianiline) confirms the existence of a tetranuclear double-stranded homotopic and unsaturated helicate. In each Cu–Gd pair, the reduced Cu···Gd distance allows ferromagnetic Cu–Gd superexchange interactions through two phenoxo oxygen atoms. Replacement of gadolinium ions by terbium ions yields the first example of a helicate behaving as a single molecule magnet (SMM).

The term helicate was introduced in 1987 by J. M. Lehn to describe a metal-containing helix.[1] A helicate contains at least two ions wrapped up and coordinated to one or more organic acyclic ligands by dative bonds.[2] The first helicates involving 3d ions, copper(II) ions, appeared earlier.[3] The first 4f helicate was described in 1992,[4] while the first structural determination of a heterobimetallic 4f–4f′ helicate appeared only a few years ago.[5] The synthesis of segmental heterotopic ligands, having bidentate and tridentate binding units able to coordinate, respectively, 3d and 4f metal ions, yielded the first example of a heterobimetallic 3d–4f helicate,[6] which was first studied by NMR and high resolution emission spectra. The X-ray crystal structure of (HHH)-$[EuZnL_3]^{5+}$ (L = 2-{6-[*N*,*N*-diethylcarbamoyl]pyridin-2-yl}-1,1′-dimethyl-5,5′-methylene-2′-(5-methylpyridin-2-yl)-bis[1*H*-benzimidazole]) confirmed the triple helical structure previously established in solution, and also confirmed that there was no direct magnetic interaction between the 3d and 4f ions.[7]

As the design of new magnetic materials based on molecules is an important research topic for chemists and physicists, we wish to report here the structural determination of the first example of a double-stranded helicate, containing two isolated Cu–Gd pairs of ions with ferromagnetic Cu–Gd interactions. Replacement of gadolinium ions by terbium ions yields the first example of a helicate behaving as a single molecule magnet (SMM). Indeed, the presence of both chirality and Ising anisotropy can lead to the observation of novel magnetochiral non-linear effects and give valuable information on the magnetic structure.

The thin platelets we isolated behaved as weakly diffracting crystals, meaning that we obtained a low resolution structure with a low diffraction Θ and an elevated R_{int}. Nevertheless, the X-ray structure determination of $[L_2Cu_2Gd_2(NO_3)_6(H_2O)_2]$-$(0.5\ H_2O)$ (**1**) (L = bis-[(2-hydroxy-3-ethoxyphenyl)methylene]-4,4′-methylenedianiline) confirms the existence of a tetranuclear double-stranded homotopic and unsaturated helicate.[8] A molecular plot of the helicate is shown in Fig. 1. Each ligand strand possesses a sequence of two similar binding units, including an imine nitrogen atom, one phenoxo and one ethoxy oxygen atom. The denticity of these binding units is not twice tridentate but twice bis-bidentate, for the central oxygen atom links the copper and gadolinium ions. If the stereochemical requirement of the copper ions can be satisfied by the presence of two strands, the gadolinium coordination sphere is not completed by four oxygen atoms. Furthermore, the two Cu–Gd pairs present in the helicate show different coordination spheres. Due to the helical arrangement of both ligands, the copper coordination sphere of the Cu1–Gd1 pair is best described as being square planar with tetrahedral distortion to the N_2O_2 donor set. But on closer examination of the structure, one nitrate anion can be considered as bridging the Cu and Gd ions with a $\eta^1:\eta^2:\mu$ mode, with a large Cu1–O bond length (2.746(9) Å). The gadolinium ion (Gd1) is ten-coordinate. In addition to the two phenoxo oxygen atoms, the lanthanide ion is also linked to an ethoxy oxygen atom from one strand. Its coordination is completed by chelation to three bidentate nitrate ions through six oxygen atoms, while the tenth one comes from a water molecule. The second Cu–Gd pair presents a different coordination mode. The copper ion is five-coordinate to the N_2O_2 donor set of the two strands in its equatorial plane and an oxygen atom from a nitrate ion bridging the Cu and Gd ions in a $\eta^1:\eta^1:\mu$ mode, with an apical Cu2–O28 bond length of 2.499(9) Å. The gadolinium ion (Gd2) is also ten-coordinate. In comparison to the Gd1 coordination sphere, the main difference originates from the replacement of an oxygen atom coming from a nitrate anion by an ethoxy oxygen atom from the second ligand strand, the other coordinated oxygen atoms being identical. Indeed, the complexation of one nitrate anion changes from being a chelating mode for Gd1 to a $\eta^1:\eta^1:\mu$ Cu–Gd bridging mode for Gd2. The Cu···Gd distances in the helicate are 3.339(2) (pair 1) and 3.425(2) Å (pair 2), respectively, while the Cu···Cu distance is 11.931(4) Å. Due to this large distance, the two Cu–Gd pairs appear to be well-separated from each other.

---

[a] *Institute of Chemistry, Academy of Sciences of Moldova, Academiei str. 3, MD-2028 Chisinau, Moldova*
[b] *Laboratoire de Chimie de Coordination du CNRS, UPR 8241, liée par conventions à l'Université Paul Sabatier et à l'Institut National Polytechnique de Toulouse, 205 route de Narbonne, 31077 Toulouse Cedex, France. E-mail: costes@lcc-toulouse.fr; Fax: +33 (0)5 61 55 30 03*
[c] *Institut Néel, CNRS & UJP, BP 166, 38042 Grenoble Cedex 9, France. E-mail: wolfgang.wernsdorfer@grenoble.cnrs.fr*

† Electronic supplementary information (ESI) available: Additional Figures (Fig. S1–S9). See DOI: 10.1039/b716283a

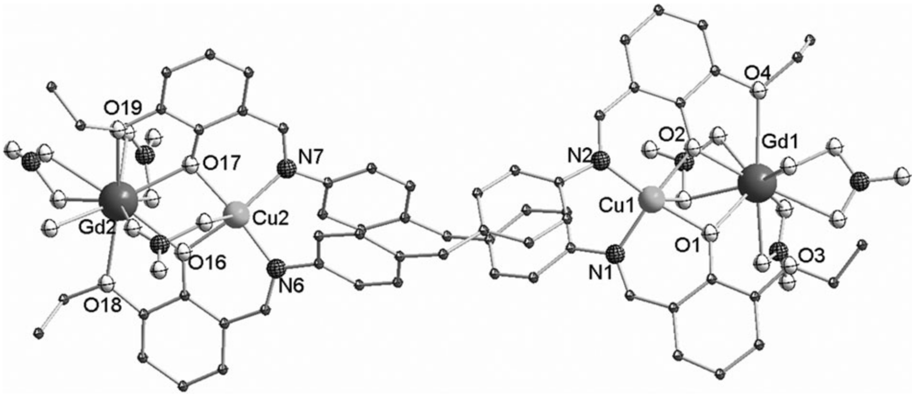

Fig. 1 Molecular structure of helicate **1**, with a partial atom labelling scheme and hydrogen atoms omitted.

Helicates **1**, **2** and **3** were characterized by MS-FAB$^+$, and **4** by MS-ESI (Fig. S1–S3†). The numbering of the different helicates is specified in the Experimental section. In each case, monocationic species were observed ([**1**, **2** or **3** − NO_3]$^+$ and [**4** − hfa]$^+$ (hfa = hexafluoroacetylacetonato ligand)). Assuming that the Cu–Gd interactions are equal within the two Cu–Gd pairs of helicate **1**, we have computed an interaction parameter, J, of 4.5 cm^{-1} by using the Hamiltonian $H = -2\{J_{\text{Cu–Gd}}(S_{\text{Cu}}S_{\text{Gd}})\}$. A corrective term θ ($\theta = -0.25$ K) was applied to take into account the $\chi_M T$ decrease at very low temperature (Fig. S4†).[8] In order to check the origin of such an interaction, we prepared complex **2** [$L_2Cu_2Y_2(NO_3)_6(H_2O)_2$]. In helicate **2**, the Gd ions were replaced by diamagnetic Y^{3+} ions, so that the Cu^{2+} ions were the only magnetic centres. Indeed the $\chi_M T$ value (0.85 cm^3 mol^{-1} K), corrected for the diamagnetism of the ligands,[9] is constant from room temperature to 20 K, while it decreases smoothly until 2 K. Fitting with a simple isotropic Hamiltonian $H = -JS_{\text{Cu1}}S_{\text{Cu2}}$ yields a J value of -0.44 cm^{-1}, with g equal to 2.13 and an agreement parameter, R, of 1×10^{-4} (Fig. S5†). The slight $\chi_M T$ decrease originates most probably from intramolecular Cu$\cdots$Cu interactions. Ferromagnetic interactions are also observed with (Cu–Tb)$_2$ helicates, as shown by the magnetization curve of **4** at 2 K (Fig. S6†).

Until now, few Cu–Tb complexes were found to behave as SMMs.[10] In order to find out whether these helicate structures were able to present SMM behaviour, ac magnetic susceptibility measurements of the corresponding Cu–Tb entities, $L_2Cu_2Tb_2(NO_3)_6(H_2O)_2$ (**3**) and $L_2Cu_2Tb_2(hfa)_6$ (**4**), were performed in the 1.8–5 K range in a 3 G ac field oscillating at 1–1500 Hz. Although the out-of-phase signals were clearly frequency-dependent, no maxima were observed (Fig. S7†). We therefore studied single crystals with a micro-SQUID setup in the 0.04–7 K range.[11]

In the case of complex **4**, magnetization (M) *vs.* applied dc field measurements revealed hysteresis loops, whose coercivity was temperature and sweep-rate dependent (Fig. 2), increasing with decreasing temperature and increasing field sweep-rate, respectively, as expected for the superparamagnetic-like behaviour of an SMM. The hysteresis loops present a very large step at zero-field, which is due to quantum tunnelling of the magnetization through the barrier. The tunnelling rates are much faster than the time scale of the applied field sweep rates, leading to a sweep rate-independent step height at the zero-field step. All molecules that do not reverse their spin at the zero-field step relax *via* a direct relaxation process at higher fields. Indeed, for SMMs with relatively large tunnel splittings, a direct relaxation process between the ground state levels becomes possible. Such hysteresis effects were observed below ~1.6 K (Fig. S8 and S9†). Because of complicating strong spin–orbit coupling of the Tb ions, we were not able to determine the anisotropy parameters.

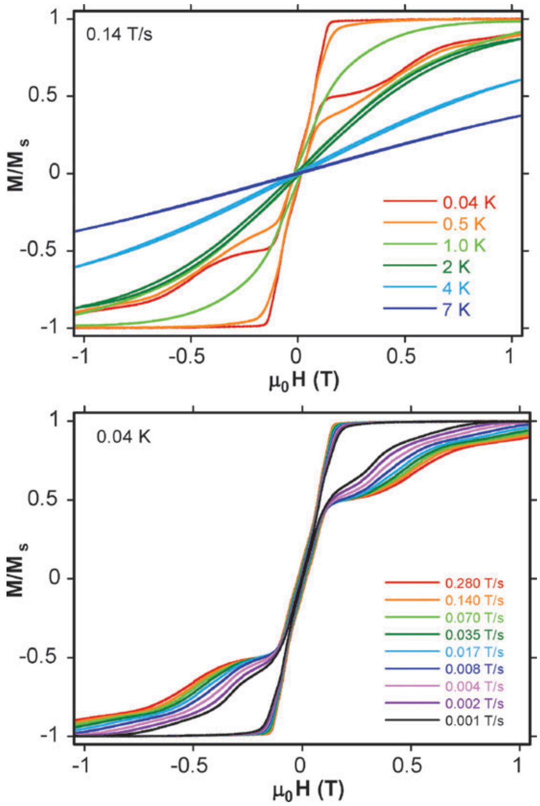

Fig. 2 Single-crystal magnetization (M) *vs.* applied field measurements (μ_0 H) for complex **4** at several temperatures (top), and for 0.04 K and several field sweep rates (bottom). M is normalised to its saturation value at 1.4 T.

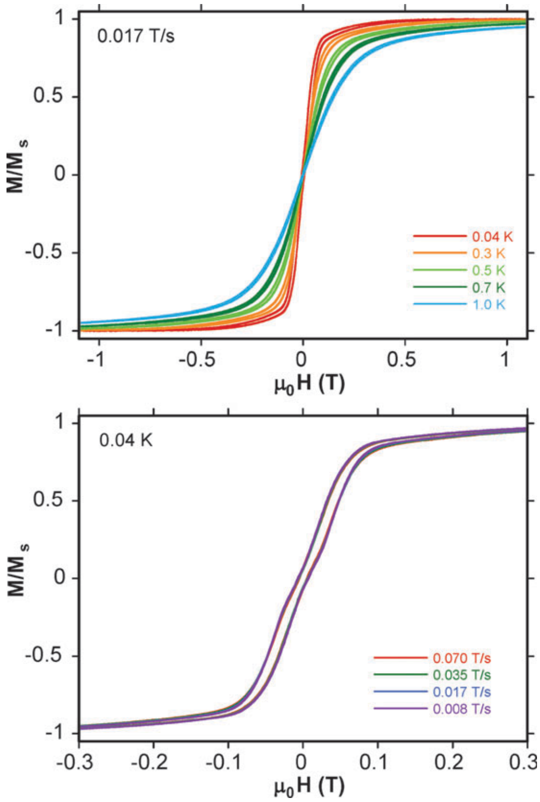

Fig. 3 Single-crystal magnetization (*M*) *vs.* applied field measurements (μ_0 *H*) for complex **3** at several temperatures (top), and for 0.04 K and several field sweep rates (bottom). *M* is normalised to its saturation value at 1.4 T.

In contrast to complex **4**, the hysteresis loops of complex **3** revealed only a very small hysteresis, which was nearly sweep rate-independent (Fig. 3). In addition, a small double-S shaped step around $H = 0$ was observed at $T = 0.04$ K, which is indicative of the presence of small antiferromagnetic interactions. The same double-S like step was observed for complex **4**, but it was less visible because of the hysteresis effect. Indeed, weak intra- and intermolecular interactions are likely to be operating in these compounds. As the hfa ligands have the advantage of giving better insulation to the helicates with respect to each other,[10] the observation of this exchange bias in complex **4** confirms the existence of intramolecular interactions in **3** and **4**.

In conclusion, the X-ray structure determination of complex **1** undoubtedly characterizes it as a heterotetranuclear unsaturated homotopic helicate. The two twice-bis-bidentate binding units of the two homotopic strands are arranged in such a way that they are able to link two different metal ions, which share the central oxygen donor atoms that transmit the magnetic interaction. This situation is responsible for the main difference from previously published 3d–4f helicates. Indeed, the first example of a 3d–4f helicate was the saturated triple-stranded (HHH)-$[EuZn(L)_3]^{5+}$ cation, in which the six- and nine-coordinated Zn and Eu ions were well-separated from each other (8.960(3) Å). In the present case, the Cu···Gd distances are reduced to 3.339(2) and 3.425(2) Å, allowing superexchange interactions through the phenoxo oxygen atoms, the copper and gadolinium ions sharing two oxygen binding sites. Replacement of gadolinium ions with anisotropic terbium ions yielded helicates that showed slow relaxation of magnetization and magnetization hysteresis loops. Studies of the relaxation and hysteresis loops established SMM behaviour, which is influenced by weak intramolecular interactions. The preparation of other Cu–Ln helicates in this series is under way, in order to complete the study of their magnetic and SMM properties.

Ghenadie Novitchi thanks the A. von Humboldt foundation for financial support.

Experimental section

The preparation of the LH_2 ligand and dinuclear copper complex have been previously described.[8] Helicates $[L_2Cu_2Gd_2(NO_3)_6(H_2O)_2](0.5\ H_2O)$ (**1**), $[L_2Cu_2Y_2(NO_3)_6(H_2O)_2]$ (**2**) and $[L_2Cu_2Tb_2(NO_3)_6(H_2O)_2]$ (**3**) were prepared by the same experimental procedure with the corresponding lanthanide salts.

1: L_2Cu_2 (0.26 g, 0.23 mmol) dissolved in acetone (150 mL) was slowly added to an acetone solution (20 mL) of $Gd(NO_3)_3 \cdot 5H_2O$ (0.23 g, 0.46 mmol) with stirring. Slow concentration of the solution yielded crystals suitable for X-ray measurements. Yield: 0.30 g (71%). Anal. calc. for $C_{62}H_{61}Cu_2Gd_2N_{10}O_{28.5}$: C, 40.4; H, 3.3; N, 7.6. Found: C, 40.0; H, 3.3; N, 7.3%. Characteristic IR absorptions (KBr): 3409, 1615, 1595, 1506, 1462, 1384, 1290, 1233, 1193, 1089, 814, 741 and 518 cm^{-1}. MS (FAB$^+$): *m*/*z* 1736 $[M - NO_3]^+$.

Crystal structure data for **1**: $C_{62}H_{61}Cu_2Gd_2N_{10}O_{28.5}$, M = 1843.78, monoclinic, space group $P2_1/n$, $a = 12.5550(16)$, $b = 30.990(3)$, $c = 18.6914(19)$ Å, $\beta = 108.095(10)°$, $V = 6912.8(13)$ Å^3, $Z = 4$, $\rho_{calc} = 1.767$ g cm^{-3}, $T = 180(2)$ K, 37 092 reflections collected, 9896 unique ($R_{int} = 0.1262$), $R = 0.0871$, w$R = 0.2323$ ($I > 2\sigma(I)$).‡

2: Yield: 0.27 g (79%). Anal. calc. for $C_{62}H_{60}Cu_2N_{10}O_{28}Y_2$: C, 43.8; H, 3.6; N, 8.2. Found: C, 43.5; H, 3.5; N, 8.0%. Characteristic IR absorptions (KBr): 3385, 1614, 1594, 1506, 1464, 1384, 1289, 1235, 1193, 1090, 814, 741 and 518 cm^{-1}. MS (FAB$^+$): *m*/*z* 1600 $[M - NO_3]^+$.

3: Yield: 0.28 g (66%). Anal. calc. for $C_{62}H_{60}Cu_2N_{10}O_{28}Tb_2$: C, 40.5; H, 3.3; N, 7.6. Found: C, 40.5; H, 3.3; N, 7.3%. Characteristic IR absorptions (KBr): 3422, 1614, 1594, 1506, 1462, 1384, 1289, 1234, 1193, 1090, 814, 741 and 518 cm^{-1}. MS (FAB$^+$): *m*/*z* 1740 $[M - NO_3]^+$.

4 $[L_2Cu_2Tb_2(hfa)_6]$: $Tb(hfa)_3 \cdot 2H_2O$ (0.3 g, 0.36 mmol)[12] was added to a dichloromethane solution of L_2Cu_2 (0.20 g, 0.18 mmol). The resulting solution was stirred at room temperature for 1 h, filtered off and evaporated. The solid was dissolved in diethyl ether; concentration of this solution yielded a brown powder, which was filtered off and dried. Yield: 0.36 g (75%). Anal. calc. for $C_{92}H_{62}Cu_2F_{36}N_4O_{20}Tb_2$: C, 41.4; H, 2.3; N, 2.1. Found: C, 41.0; H, 2.2; N, 2.0. Characteristic IR absorptions (KBr): 1654, 1615, 1596, 1555, 1506, 1465, 1255, 1194, 1144, 1099, 796, 739, 660 and 584 cm^{-1}. MS (ESI): *m*/*z* 2466.4 $[M - hfa]^+$.

References

‡ CCDC 649306. For crystallographic data in CIF or other electronic format see DOI: 10.1039/b716283a

1 (*a*) J.-M. Lehn, A. Rigault, J. Siegel, J. Harrowfield, B. Chevrier and D. Moras, *Proc. Natl. Acad. Sci. U. S. A.*, 1987, **84**, 2565; (*b*) J.-M. Lehn, *Supramolecular Chemistry: Concepts and Perspectives*, VCH, Weinheim, Germany, 1995; (*c*) J.-M. Lehn, *Science*, 2002, **295**, 2400.

2 (*a*) C. Piguet, G. Bernardinelli and G. Hopfgartner, *Chem. Rev.*, 1997, **97**, 2005; (*b*) J. Malina, M. J. Hannon and V. Brabec, *Chem.–Eur. J.*, 2007, **13**, 3871; (*c*) J. Muller and B. Lippert, *Angew. Chem., Int. Ed.*, 2006, **45**, 2503; (*d*) M. Pascu, G. J. Clarkson, B. M. Kariuki and M. J. Hannon, *Dalton Trans.*, 2006, 2635; (*e*) A. Lavalette, F. Tuna, G. Clarkson, N. W. Alcock and M. J. Hannon, *Chem. Commun.*, 2003, 2666; (*f*) P. Cucos, M. Pascu, R. Sessoli, N. Avarvari, F. Pointillart and M. Andruh, *Inorg. Chem.*, **45**, 7035; (*g*) O. Mamula, M. Lama, S. G. Telfer, A. Nakamura, R. Kuroda, H. Stoeckli-Evans and R. Scopelitti, *Angew. Chem., Int. Ed.*, 2005, **44**, 2527.

3 (*a*) C. M. Harris and E. D. McKenzie, *J. Chem. Soc. A*, 1969, 746; (*b*) C. J. Carrano and K. N. Raymond, *J. Am. Chem. Soc.*, 1978, **100**, 5371.

4 G. Bernardinelli, C. Piguet and A. F. Williams, *Angew. Chem., Int. Ed. Engl.*, 1992, **31**, 1622.

5 N. André, R. Scopelliti, G. Hopfgartner, C. Piguet and J.-C. G. Bünzli, *Chem. Commun.*, 2002, 214.

6 C. Piguet, E. Rivara-Minten, G. Hopfgartner and J.-C. G. Bünzli, *Helv. Chim. Acta*, 1995, **78**, 1541.

7 C. Piguet, G. Bernardinelli, J.-C. G. Bünzli, S. Petoud and G. Hopfgartner, *J. Chem. Soc., Chem. Commun.*, 1995, 2575.

8 Gh. Novitchi, J. P. Costes and J. P. Tuchagues, *Dalton Trans.*, 2004, 1739.

9 P. Pascal, *Ann. Chim. Phys.*, 1910, **19**, 5.

10 (*a*) S. Osa, T. Kido, N. Matsumoto, N. Re, A. Pochaba and J. Mrozinski, *J. Am. Chem. Soc.*, 2004, **126**, 420; (*b*) J. P. Costes, M. Auchel, F. Dahan, V. Peyrou, S. Shova and W. Wernsdorfer, *Inorg. Chem.*, 2006, **45**, 1924; (*c*) J. P. Costes, F. Dahan and W. Wernsdorfer, *Inorg. Chem.*, 2006, **45**, 5.

11 W. Wernsdorfer, *Adv. Chem. Phys.*, 2001, **118**, 99.

12 M. F. Richardson, W. F. Wagner and D. E. Sands, *J. Inorg. Nucl. Chem.*, 1968, **30**, 1275.